ENGINEERING JOURNAL

Article

Zirconia Modification on Nanocrystalline Titania-Supported Cobalt Catalysts for Methanation

Kitima Pinkaew [1], **Okorn Mekasuwandumrong**[2], **Joongjai Panpranot**[1], **Artiwan Shotipruk**[1], **Piyasan Praserthdam**[1], **James G. Goodwin, Jr.**[3], **and Bunjerd Jongsomjit**[1],*

1 Center of Excellence on Catalysis and Catalytic Reaction Engineering, Department of Chemical Engineering, Faculty of Engineering, Chulalongkorn University, Bangkok 10330, Thailand
2 Department of Chemical Engineering, Faculty of Engineering and Industrial Technology, Silpakorn University, Nakhon Pathom 73000, Thailand
3 Department of Chemical Engineering, Clemson University, Clemson, South Carolina 29634, USA
E-mail: bunjerd.j@chula.ac.th*

Abstract. In this present study, the zirconia-modified TiO_2 having different crystallite sizes of 11, 13 and 16 nm as support for the cobalt catalysts were investigated. The different TiO_2 crystallites derived from the sol-gel method was obtained by varying the water:alkoxide molar ratios from 165 to 4. Then, the TiO_2 supports were used to yield various Co/TiO_2 catalysts. It was found that the sizes of cobalt oxides species dispersed on TiO_2 were corresponding to TiO_2 sizes. Based on XPS study, the binding energy of Co $2p_{3/2}$ was not affected by the size of TiO_2. The catalytic activity was measured via CO hydrogenation under methanation condition. In case of unmodified TiO_2 support, the smaller TiO_2 crystallites (Co/TiO_2_11 nm) exhibited higher activity than other larger ones. Moreover, the zirconia modification also resulted in increased activity for all samples. For both cases, it can be attributed to the increased cobalt dispersion with small crystallite size of TiO_2 support coupled with the zirconia modification as measured by CO chemisorption.

Keywords: nanocrystalline TiO_2, sol-gel; cobalt catalyst, methanation, CO hydrogenation.

1. Introduction

The Fischer-Tropsch (FT) synthesis was successfully carried out for future alternative resource instead of coal or crude oil. There are many active metals such as Ru, Fe, Co, Pd, and etc. that can be used for hydrogenation of carbon monoxide (CO) to long chain hydrocarbon. For example, cobalt and iron are the metals which have been used in the industry for hydrocarbon synthesis. Even though, the cobalt catalysts are more expensive, they are more resistant to deactivation than iron metals [1]. Supported cobalt catalysts have been extensively investigated with many inorganic supports for years, such as SiO_2 [2], Al_2O_3 [3], TiO_2 [4]. Supported cobalt catalysts, which are the most popular FT catalysts, have been used as catalyst for FT synthesis for many years because of their high catalytic activity and selectivity [5]. CO and H_2 (syngas) have been converted to paraffinic or long chain hydrocarbon through hydrogenation reaction. In fact, the interaction between cobalt oxide species and supports has an important role on dispersion of cobalt oxide species [6]. As known, the catalytic performance is usually enhanced by addition a promoter such as noble metal or metal oxide. The oxide promoter, such as zirconia (ZrO_2) has been employed to improve the activity and hydrocarbon selectivity of cobalt catalysts. The oxide promoters could modify the catalyst properties, increase cobalt dispersion, reducibility, and improve the chemical stability of the support. For instance, it was found that the promotion with zirconia resulted in higher activity in FT reaction rates [7].

Due to the significant development in nanotechnology in the recent years, many inorganic nanomaterials have brought much attention to the research in heterogeneous catalysis. These inorganic nanomaterials can be potentially used as supports for catalytic phase because of their unique properties, great thermal and mechanical stability. In the present work, the nanocrystalline TiO_2 having different crystallite sizes was prepared via the sol-gel method and used as support for Co catalysts. The different TiO_2 nanocrystallites were prepared by varying the water:alkoxide molar ratio during sol-gel synthesis, and then they were modified with zirconia. Thus, the effects of crystallite size coupled with the zirconia modification of the TiO_2 supports on the properties of Co catalysts are elucidated. The characteristics of different supports and catalysts were determined by means of several techniques, such as X-ray diffraction (XRD), scanning electron microscopy (SEM) and energy dispersive X-ray spectroscopy (EDX), transmission electron microscope (TEM), carbon monoxide (CO) chemisorption, and X-ray photoelectron spectroscopy (XPS). The activity and product selectivity of catalysts were measured via CO hydrogenation under methanation condition to minimize the catalyst deactivation.

2. Experimental

2.1. Preparation of Nanocrystalline TiO_2

TiO_2 was prepared by the sol-gel method [8]. First, the titania precursor [titanium (IV) isopropoxide] was dissolved in ethanol (125 mL), and then mixed with the solution of water:alkoxide having molar ratios between 4 to 165 in order to obtain different crystallite sizes of TiO_2. The mixture was added dropwise to the aqueous solution with stirring by ultrasonic at room temperature. The mixture was stirred for 2 h. The obtained amorphous precipitates were centrifuged and redispersed in ethanol five times prior to filtration. After that, the sample was dried and calcined at 450°C in air flow for 2 h.

2.2. Preparation of Zr-Modified TiO_2

The Zr-modified TiO_2 support was prepared by the incipient wetness impregnation having 0.3 wt% of Zr. The desired amount of zirconium (IV) n-propoxide 70 wt% solution in 1-propanol was dissolved in deionized water, and then was dropped slowly onto the TiO_2 support. The modified support was dried at 110°C for 12 h and calcined in air at 350°C for 2 h [9].

2.3. Preparation of Cobalt Catalyst

A 20 wt% of Co metal was impregnated onto the TiO_2 supports obtained from sections 2.1 and 2.2 using cobalt nitrate [$Co(NO_3)_2 \cdot 6H_2O$] as a precursor . The sample was dried at 110°C for 12 h and calcined in air at 500°C for 4 h in order to convert all cobalt nitrate precursors into Co oxide species.

The nomenclature used for the catalyst samples in this study is as follows:

- Co/TiO$_2$_xx nm
- Co/TiO$_2$_xx nm_Zr

Co/TiO$_2$_ xx nm refers to Co/TiO$_2$ catalyst using TiO$_2$ having the crystallite size of xx nm, and Co/TiO$_2$_xx nm_Zr refers to the Co/TiO$_2$ catalyst using TiO$_2$ having the crystallite size of xx nm with Zr modification on TiO$_2$.

2.4. Methanation

CO hydrogenation (H$_2$/CO = 10/1) under methanation condition was performed to determine the overall activity of the samples. Hydrogenation of CO was carried out at 220°C and 1 atm. A flow rate of H$_2$/CO/Ar = 20/2/8 cm^3/min in a fixed-bed flow reactor was used. A relatively high H$_2$/CO ratio was used to minimize deactivation due to carbon deposition during reaction. Typically, 10 mg of a sample was reduced *in situ* in flowing H$_2$ (30 cm^3/min) at 350°C for 10 h prior to the reaction. Reactor effluent samples were taken at 30-min intervals and analyzed by GC. Thermal conductivity detector (TCD) with molecular sieve 5 Å was used to detect the CO. A flame ionization detector (FID) with a VZ-10 column was used to detect the light hydrocarbons, such as C$_1$-C$_4$ hydrocarbons. In all cases, steady-state was reached within 5 h.

2.5. Characterization of Support and Catalyst

2.5.1.   N$_2$ Physisorption

The surface area was determined by physisorption of nitrogen using a micromeritics pulse chemisorb 2700 system. It was calculated based on nitrogen uptake at liquid-nitrogen temperature (-196°C) using the Brunauer-Emmett-Teller (BET) equation by the single point method.

2.5.2.   X-ray Diffraction

XRD was performed to determine the bulk crystalline phases of the sample. It was conducted using a SIEMENS D-5000 X-ray diffractometer with Cu K$_\alpha$ (λ = 1.54439 $\overset{\circ}{A}$). The spectra were scanned at a rate of 2.4°/min in the range 2θ = 20–80°.

2.5.3.   Scanning Electron Microscopy and Energy Dispersive X-ray Spectroscopy

SEM and EDX were used to determine the catalyst morphologies and elemental distribution throughout the sample granules, respectively. SEM was carried out using a JEOLmodel JSM-5800LV. EDX was performed using Link Isis series 300 program.

2.5.4.   Transmission Electron Microscopy

TEM was used to determine the dispersion of cobalt oxide species using JEOL-TEM 200CX transmission electron spectroscopy operated at 100 kV with 50k magnification. The sample was dispersed in ethanol to obtain the uniform dispersion of sample prior to the measurement.

2.5.5.   X-ray Photoelectron Spectroscopy

XPS was used to examine the binding energy of the catalysts by using an AMICUS spectrometer with X-ray source of Mg K$_\alpha$ radiation operated at voltage of 20 kV, current of 10 mA using the AMICUS "VISION2" software.
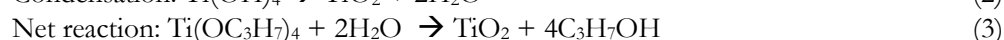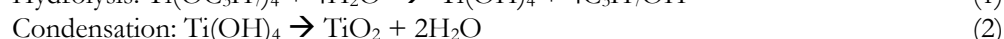
2.5.6.   CO Chemisorption

The active sites and the relative percentage dispersion of cobalt catalyst were determined by CO-pulse chemisorption technique using Micromeritics ChemiSorb 2750 (pulse chemisorption system) and ASAP 2101C V.3.00 software. It was carried out using 20 mg of a sample and reduced in H$_2$ at 50 ml/min upon

heating from room temperature to 350°C at 10°C/min and held at this temperature for 3 h, and then cooled down to room temperature in a He flow. Gas volumetric chemisorption at 100°C was performed. Desorbed CO was measured using thermal conductivity detector. Pulsing was continued until no further carbon monoxide adsorption was observed.

3. Results and Discussion

3.1. Characteristics

First, the crystallite size of the sol-gel derived TiO_2 was varied by changing the water:alkoxide molar ratios (three values from 4, 40, and 165) during the synthesis. In this sol-gel process, the reaction between the alkoxide precursor and the desired amount of water occurred in an anhydrous alcohol medium. The hydrolysis and condensation reactions can be summarized as follows [10]:

$$\text{Hydrolysis: } Ti(OC_3H_7)_4 + 4H_2O \rightarrow Ti(OH)_4 + 4C_3H_7OH \tag{1}$$
$$\text{Condensation: } Ti(OH)_4 \rightarrow TiO_2 + 2H_2O \tag{2}$$
$$\text{Net reaction: } Ti(OC_3H_7)_4 + 2H_2O \rightarrow TiO_2 + 4C_3H_7OH \tag{3}$$

As seen from the net reaction (3), the nucleation rate of TiO_2 increases with increasing the water:alkoxide ratios. As a result, the crystallite size and nanoparticle size should decrease with increasing the water:alkoxide ratios. After calcination, the obtained TiO_2 supports were characterized using XRD and N_2 physisorption. It was found that all three samples exhibited the similar XRD patterns (not shown) at 26°(major), 37°, 48°, 55°, 56°, 62°, 69°, 71°, and 75° assigned to the TiO_2 in the anatase phase. The crystallite sizes of TiO_2 were calculated based on the XRD line broadening using the Scherrer equation. It was found that the crystallite sizes of TiO_2 were in the range of 11, 13 and 16 nm corresponding to the water:alkoxide ratios of 165, 40 and 4, respectively. It appeared that increased water:alkoxide molar ratio apparently resulted in decreased crystallite size of TiO_2. The BET surface areas of samples were found to be 71, 63 and 48 m²/g for TiO_2_11 nm, TiO_2_13 nm, and TiO_2_16 nm, respectively, which were usual for anatase TiO_2 obtained from the sol-gel method. After Zr modification of the TiO_2 supports, it showed only a slight decrease in surface area. No XRD peaks of Zr were detected due to its highly dispersed form.

After impregnation of Co onto the different TiO_2 supports as mentioned above, the catalysts were calcined and characterized using various techniques. The XRD patterns for the calcined catalyst samples without Zr modification are shown in Fig. 1. Besides the appearance of XRD patterns of the anatase TiO_2 as mentioned above, all calcined samples exhibited XRD peaks at 31° (weak), 36° (strong), 46° (weak), and 65° (weak), which were assigned to the presence of Co_3O_4 species. No other forms of Co oxide species can be detected by the XRD measurement. The XRD patterns for the calcined catalyst samples with Zr modification (not shown) were also similar to those without Zr modification.

The surface areas of the catalysts with and without Zr modification are also shown in Table 1. They slightly decreased with Zr modification. It should be noted that high surface area could result in better distribution of Co, but somehow does not guarantee good dispersion as shown in our previous work [11]. The crystallite sizes of Co_3O_4 were also shown in Table 1. It indicated that the Zr modification can result in increased crystallite size of Co_3O_4 on TiO_2 supports. In order to determine the Co dispersion and active sites, the CO chemisorption was performed as shown in Table 1. Apparently, the Co dispersion increased with Zr modification on the support. This phenomenon was in agreement with Feller *et al.* [7] when Zr was co-impregnated with cobalt onto the silica support.
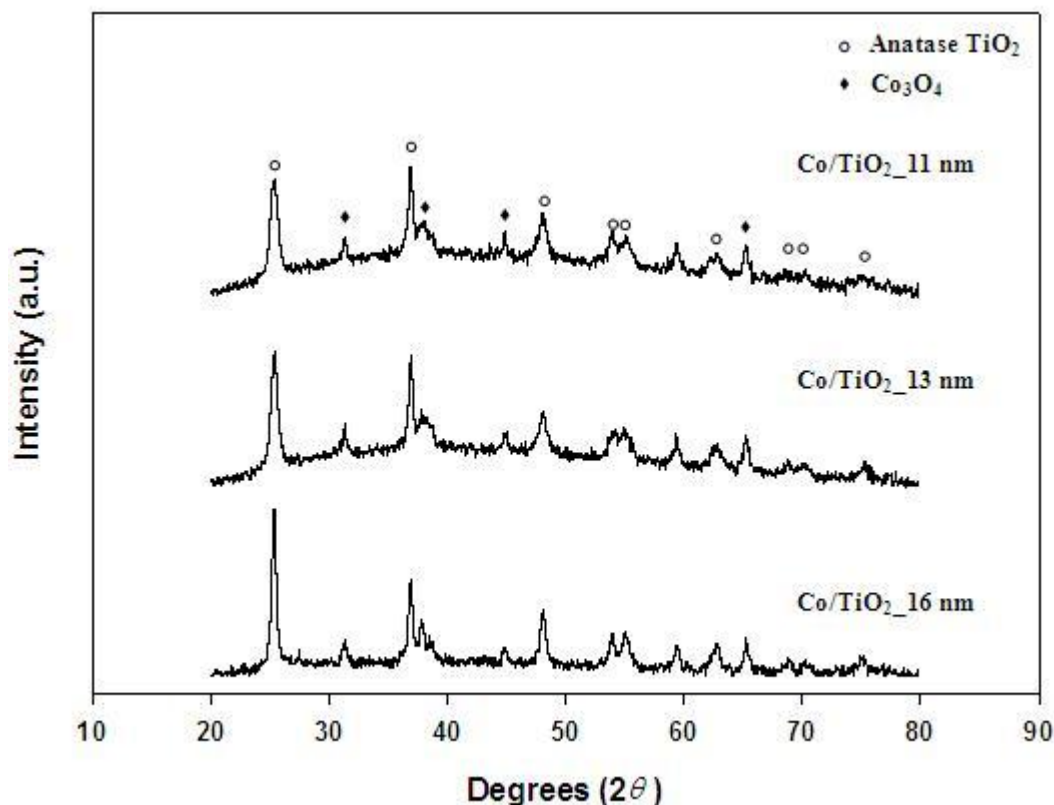
Fig. 1.   XRD patterns for Co catalysts with different crystallite sizes of TiO_2 support.

Table 1.   Characteristics of catalyst samples.

Samples	Surface Area (m²/g)	Crystallite Size of Co_3O_4 (nm)[a]	CO Chemisorption	
			CO Chemisorption (μmole CO/g cat)	Co^0 Dispersion[b] (%)
Co/TiO₂_11 nm	52	11	23.1	3.5
Co/TiO₂_13 nm	40	14.9	21.4	3.3
Co/TiO₂_16 nm	10	19.5	6.7	1.0
Co/TiO₂_11 nm_Zr	40	17.3	29.0	4.3
Co/TiO₂_13 nm_Zr	32	20.3	23.4	3.5
Co/TiO₂_16 nm_Zr	12	24.8	9.5	1.4

[a]*Calculated based on XRD line broadening using Scherrer Equation.*
[b]*Calculated based on fraction of Co^0 detected from CO chemisorption per Co^0 loading x 100.*

The morphologies and elemental distribution of the catalyst samples were determined using SEM and EDX, respectively. The SEM micrograph for all catalyst samples are illustrated in Fig. 2. It can be seen that the larger crystallite sizes of TiO_2 support can result in more agglomeration of catalyst particles. The EDX mapping for all samples (not shown) also revealed well distribution of cobalt on the support granules.
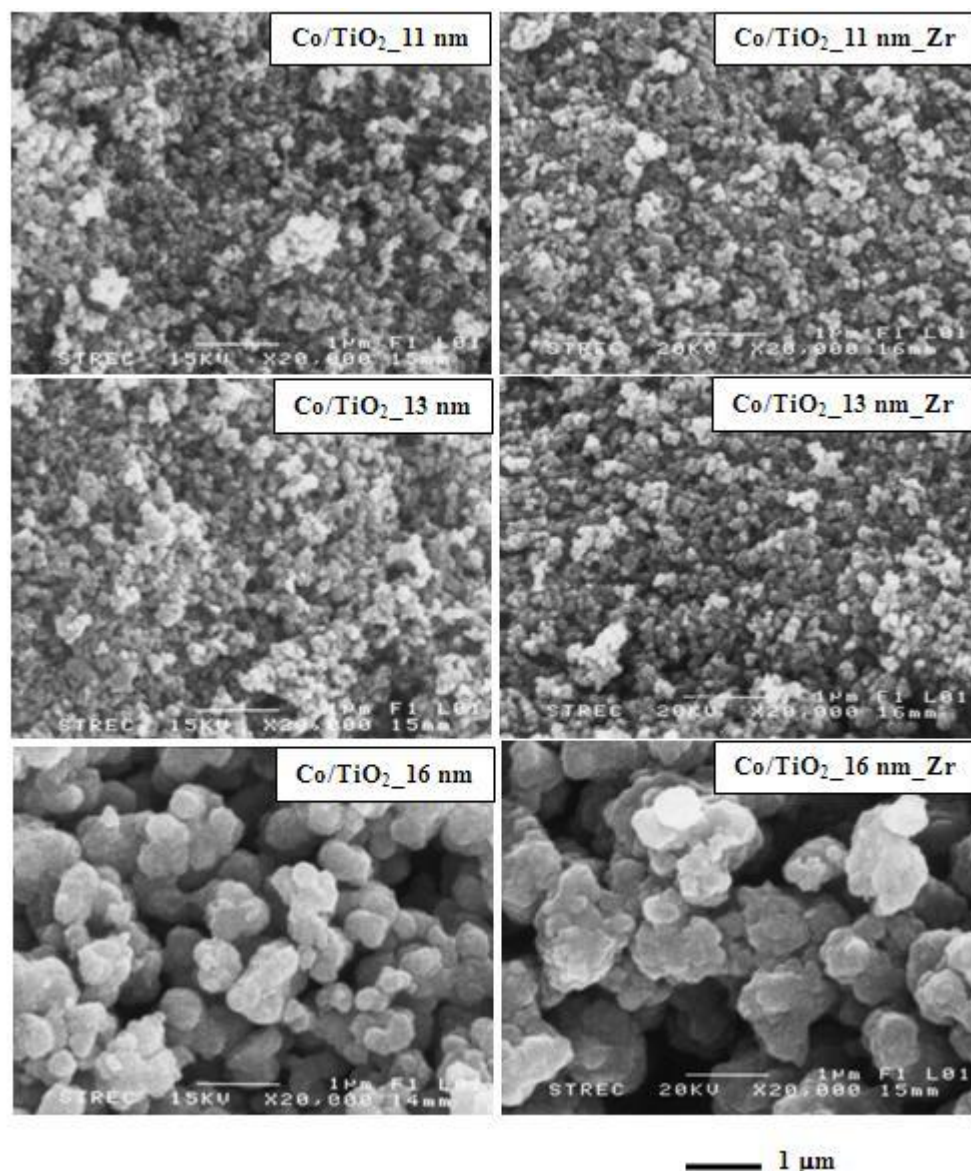
Fig. 2.   SEM micrographs of Co catalysts with and without Zr-modified different crystallite sizes of TiO_2 supports.

    In order to determine the dispersion of cobalt oxide species on the different TiO_2 supports, a more powerful technique, such as TEM was applied for all samples. The TEM micrographs of all catalysts are shown in Fig. 3. The dark spots represent cobalt oxide species dispersed on the different TiO_2 supports. The TEM micrographs of the catalyst using smaller crystallite size of TiO_2 exhibited the better dispersion than the larger one indicating the smaller size of cobalt oxide species. It is suggested that the dispersion of cobalt oxide species could be altered by the size of support used as also mentioned in our previous work [12]. In addition, the Zr modification on TiO_2 supports showed the similar appearance to those without Zr modification. However, they were more agglomerated.   These results were in accordance with those obtained from the XRD measurement, where the crystallite sizes of cobalt oxides species were larger with the Zr modification as shown in Table 1.
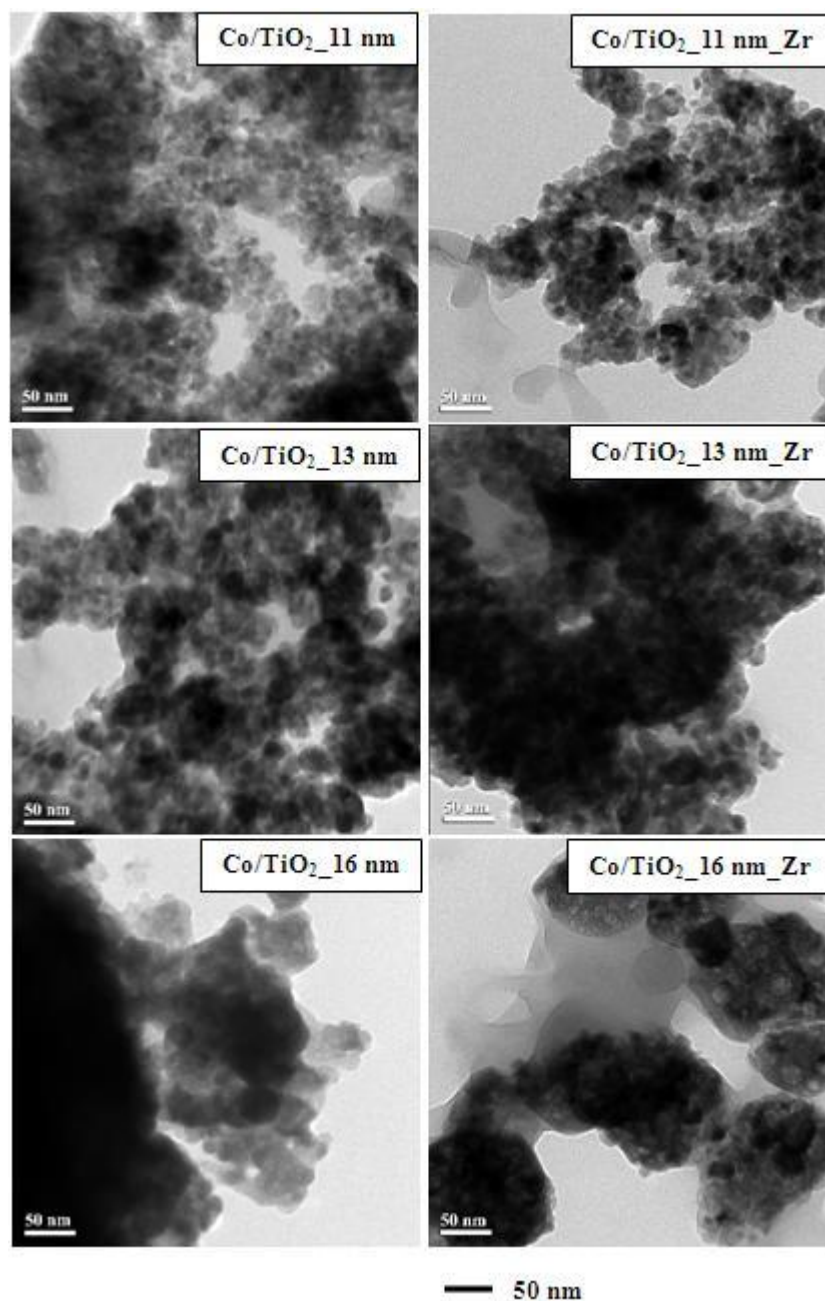
Fig. 3. TEM micrographs of Co catalysts with and without Zr-modified different crystallite sizes of TiO$_2$ supports.

Hence, it indicated that the larger size of cobalt oxides species was favorable with Zr modification to obtain the high dispersed cobalt metal surface atoms as measure by CO chemisorption, listed in Table 1. This is suggested that the Zr modification may result in increased interaction of cobalt oxide species with the support, thus promoting the reduction of larger crystallites. It is worth noting that the Zr modification was more pronounced on the larger TiO$_2$ crystallites.

The XPS analysis was carried out to examine the binding energy of species on the catalysts. The catalyst samples were analyzed in the Co 2p, Ti 2p, O 1s, Zr 3d with regards to the binding energy regions. The peaks of Zr 3d would be detected around 179.2 eV [13], but there was no observation of the Zr 3d due to very small amount of Zr loading. The binding energy values corresponding to Co 2p and Ti 2p were not affected by the small amount of Zr modification with the values of ca. 780 eV and 459 eV, respectively.

3.2. Reaction study

The reaction study was carried out via CO hydrogenation under methanation condition in order to minimize the catalyst deactivation due to carbon deposition. The conversion, reaction rate and product selectivity for all samples are shown in Table 2.

Table 2.   Reaction study.

Samples	Conversion (%)	SS Rate ($x10^2$ gCH$_2$/g cat.h)	Product Selectivity (%)	
			C$_1$	C$_2$-C$_4$
Co/TiO$_2$_11 nm	77	28.9	97	3
Co/TiO$_2$_13 nm	49	18.4	94	6
Co/TiO$_2$_16 nm	32	12.0	94	6
Co/TiO$_2$_11 nm_Zr	100	37.5	98	2
Co/TiO$_2$_13 nm_Zr	83	31.2	97	3
Co/TiO$_2$_16 nm_Zr	90	33.8	99	1

The CO conversion was ranged between 32 and 100% upon different TiO$_2$ supports. Based on the reaction rates, it is obvious that the activities of catalysts decreased with increasing the crystallite size of TiO$_2$ support from 11 to 16 nm due to decreased Co dispersion. In addition, Zr modification apparently resulted in increased activity for all different crystallite sizes of TiO$_2$ supports. However, the Zr modification had more pronounced effect on the larger crystallite size support where the conversion increased about two times. This can be attributed to the promotion of cobalt dispersion by Zr. It is worth noting that Zr can be added into the Co catalyst as a promoter by coimpregnation with the cobalt precursor, such as cobalt nitrate. Considering the product selectivity, it was found that in all cases, methane was present as a majority product, which is typical for CO hydrogenation under methanation. Without Zr modification, the catalysts having larger crystallite size of TiO$_2$ trended to give more amounts of longer chain hydrocarbons (C$_2$-C$_4$).   However, the C$_2$-C$_4$ decreased with the Zr promotion. It is known that CO hydrogenation is a kind of polymerization reactions where insertion of the –CH$_2$- (methylene group) occurs through the active centers [14], rate of propagation, and rate of termination. Obviously, the termination of chain growth occurs and is recognized as the chain growth probability. Based on product selectivity found here, it can be concluded that the Zr modification in TiO$_2$ supports slightly inhibited the chain growth probability.   As a mater of fact, it resulted in the observation of higher methane selectivity with Zr modification.

4. Conclusion

Based on this study, the effects of different crystallite sizes of TiO$_2$ supports on the catalytic properties of Co/TiO$_2$ catalysts were elucidated. It was found that the smaller crystallite size of TiO$_2$ support exhibited higher catalytic activity due to higher Co dispersion. The crystallite sizes of cobalt oxide species were replicated by those of the TiO$_2$ support. It also revealed that the Zr modification on the support enhanced the activity of catalysts. This can be attributed to reduction of more cobalt oxides species. It was found that the Zr modification was more pronounced on the large TiO$_2$ crystallites. The Zr promotion can result in slightly decreased C$_2$-C$_4$ hydrocarbons during methanation.

Acknowledgement

References

[1] A. Y. Khodakov, W. Chu, and P. Fongarland, "Advances in the development of novel cobalt Fischer-Tropsch catalysts for synthesis of long-chain hydrocarbons and clean fuels," *Chem. Rev.*, vol. 107, pp. 1692-1744, 2007.

[2] K. Okabe, X. Li, M. Wei, and H. Arakawa, "Fischer–Tropsch synthesis over Co-SiO$_2$ catalysts prepared by the sol–gel method," *Catal. Today*, vol. 89, pp. 431-438, 2004.

[3] A. Kogelbauer, J. G. Goodwin, Jr., and R. Oukaci, "Ruthenium promotion of Co/Al$_2$O$_3$ Fischer–Tropsch catalysts," *J. Catal.*, vol. 160, pp. 125-133, 1996.

[4] S. J. Tauster, S. C. Fung, and R. L. Garten, "Strong metal-support interactions: Group 8 noble metals supported on TiO$_2$," *J. Am. Chem. Soc.*, vol. 100, pp. 170-175, 1978.

[5] B. Jongsomjit and J. G. Goodwin, Jr., "Co-support compound formation in Co/Al$_2$O$_3$ catalysts: Effect of reduction gas containing CO," *Catal. Today*, vol. 77, pp. 191-204, 2002.

[6] S. L. Soleda, E. Iglesia, R. A. Fiatoa, J. E. Baumgartnera, H. Vromana, and S. Miseoa, "Control of metal dispersion and structure by changes in the solid-state chemistry of supported cobalt Fischer–Tropsch catalysts," *Topics Catal.*, vol. 26, pp. 101-109, 2003.

[7] A. Feller, M. Claeys, and E. V. Steen, "Cobalt cluster effects in zirconium promoted Co/SiO$_2$ Fischer-Tropsch catalysts," *J. Catal.*, vol. 185, pp. 120-130, 2001.

[8] K. Suriye, P. Praserthdam, and B. Jongsomjit, "Impact of Ti^{3+} present in titania on characteristics and catalytic properties of the Co/TiO$_2$ catalyst," *Ind. Eng. Chem. Res.*, vol. 44, pp. 6599-6604, 2005.

[9] T. Wongsalee, B. Jongsomjit, and P. Praserthdam, "Effect of zirconia-modified titania consisting of different phases on characteristics and catalytic properties of Co/TiO$_2$ catalysts," *Catal. Lett.*, vol. 108, pp. 55-61, 2006.

[10] K. V. Baiju, S. Shukla, K. S. Sandhya, J. James, and K. G. K. Warrier, "Photocatalytic activity of sol-gel-derived nanocrystalline titania," *J. Phys. Chem. C*, vol. 111, pp. 7612-7622, 2007.

[11] B. Jongsomjit, T. Wongsalee, and P. Praserthdam, "Catalytic behaviors of mixed TiO$_2$-SiO$_2$-supported cobalt Fischer–Tropsch catalysts for carbon monoxide hydrogenation," *Mater. Chem. Phys.*, vol. 97, pp. 343-350, 2006.

[12] N. Burakorn, P. Panpranot, O. Mekasuwandumrong, C. Chaisak, P. Praserthdam, and B. Jongsomjit, "Characterization of cobalt dispersed on the mixed nano-Al$_2$O$_3$-ZrO$_2$ support," *J. Mater. Proc. Tech.*, vol. 206, pp. 352-358, 2008.

[13] S. Badrinarayanant and S. Sinha, "An XPS study of the nitrogen-implanted Zr$_{76}$Fe$_{24}$ metglass," *Condens. Mater. Phys.*, vol. 2, pp. 8721-8724, 1990.

[14] B. Jongsomjit, S. Kittiruangrayub, and P. Praserthdam, "Study of cobalt dispersion onto the mixed nano-SiO$_2$-ZrO$_2$ supports and its application as a catalytic phase," *Mater. Chem. Phys.*, vol. 105, pp. 14-19, 2007.